N·H

ELSEVIER

Physics Letters B 532 (2002) 29–36

www.elsevier.com/locate/npe

Alpha decay of ^{114}Ba ☆

C. Mazzocchi [a,b], Z. Janas [a,c], L. Batist [d], V. Belleguic [a], J. Döring [a], M. Gierlik [c], M. Kapica [a], R. Kirchner [a], G.A. Lalazissis [e,f], H. Mahmud [g], E. Roeckl [a], P. Ring [f], K. Schmidt [g], P.J. Woods [g], J. Żylicz [c]

[a] *Gesellschaft für Schwerionenforschung mbH, D-64291 Darmstadt, Germany*
[b] *University of Milan, I-20133 Milan, Italy*
[c] *Institute of Experimental Physics, University of Warsaw, PL-00681 Warsaw, Poland*
[d] *St. Petersburg Nuclear Physics Institute, 188-350 Gatchina, Russia*
[e] *Physics Department, Aristotele University of Thessaloniki, GR-54006, Thessaloniki, Greece*
[f] *Physics Department, Technical University Munich, D-85748 Garching, Germany*
[g] *Department of Physics and Astronomy, University of Edinburgh, Edinburgh EH9 3JZ, United Kingdom*

Received 24 October 2001; received in revised form 14 February 2002; accepted 28 February 2002

Editor: V. Metag

Abstract

The neutron-deficient isotope ^{114}Ba was produced through the ^{58}Ni(^{58}Ni, $2n$) reaction, separated as a ^{114}Ba^{19}F^{+} beam, implanted into a stopper foil, and studied by using silicon-detector telescopes for decay spectroscopy. We measured for the first time the α-particle energy (3410 ± 40 keV) of ^{114}Ba, the half-life (160^{+290}_{-60} ms) of its daughter nucleus ^{110}Xe, and the α-decay branching ratios and widths for these two isotopes. The Q values resulting for α-decay, the Q value for ^{12}C decay of ^{114}Ba and the α-decay widths are discussed in comparison with theoretical predictions. The search for ^{113}Ba yielded a negative result.

PACS: 23.60.+e; 27.60.+j; 21.10.Tg

Keywords: Radioactivity ^{114}Ba, ^{110}Xe, ^{106}Te (from ^{58}Ni(^{58}Ni, xn)); Measured $T_{1/2}$, E_α, I_α; Deduced Q values for α and ^{12}C decay; Search for ^{113}Ba; On-line mass separation; Si detectors; Nuclear structure ^{114}Ba, ^{110}Xe, ^{106}Te, ^{102}Sn; Calculated Q values; Reduced widths

1. Introduction

One of the particularly interesting features of nuclear structure in the region near the doubly-magic nucleus ^{100}Sn ($Z = N = 50$) is the occurrence of an island of α emission, covering neutron-deficient isotopes from tellurium ($Z = 52$) to cesium ($Z = 55$). In recent years, intense experimental and theoretical research has focused on investigating these nuclei. This research included, e.g., measurements (and predictions) of masses, of direct proton and α decay-modes and of their branching ratios. The interest in the interplay between microscopic (shell) and macroscopic (liquid-drop) effects in this rather unexplored region

☆ This work is part of the Ph. D. thesis of C. Mazzocchi.
E-mail address: e.roeckl@gsi.de (E. Roeckl).

0370-2693/02
PII: S0370-2693(02)01543-5

of the nuclear chart has also stimulated recent developments in the technology of production of secondary (exotic) ion beams.

Alpha emission is a rich source for nuclear-structure information [1], in particular, for the $0^+ \to 0^+$ transitions between even-even nuclei. The α-particle energies E_α, corrected for the recoil effect, yield the difference between the ground-state masses of mother and daughter nuclides. Above ^{100}Sn, this quantity directly relates to the $Z = N = 50$ shell strength. Moreover, data on E_α, total half-life ($T_{1/2}$) and α-decay branching ratio (b_α) yield the reduced widths for this disintegration mode. These widths may shed light on the question whether superallowed α-decay [2] occurs for nuclei beyond ^{100}Sn, with protons and neutrons being in identical $d_{5/2}$, $d_{3/2}$ and $g_{7/2}$ orbitals.

Theoretical predictions [3,4] have suggested a new island of cluster radioactivity beyond the doubly-magic nucleus ^{100}Sn, the most promising candidate in this region being ^{12}C emission from ^{114}Ba [5–7]. Theoretical predictions for the partial half-life for ^{12}C emission [5,7,8] depend dramatically on the Q value ($Q_{^{12}\mathrm{C}}$): a variation of 2 MeV in $Q_{^{12}\mathrm{C}}$ results in about five orders of magnitude spread in the partial half-life. Since mass models [9–11] predict $Q_{^{12}\mathrm{C}}$ values that range from about 18 MeV to about 22 MeV, the experimental determination of $Q_{^{12}\mathrm{C}}$ for ^{114}Ba is important in planning measurements of this decay mode. The $Q_{^{12}\mathrm{C}}$ value of ^{114}Ba can be experimentally established by measuring the α-decay Q-value (Q_α) for ^{114}Ba and adopting the known Q_α for the daughter and granddaughter nuclei ^{110}Xe and ^{106}Te.

Following the early α-decay work on tellurium-to-cesium isotopes (see, e.g., [1]), new perspectives for studying light barium isotopes and their daughter activities have recently been opened, when the method of extracting barium isotopes as molecular ions from an ion source became available [12–14] at the GSI on-line mass separator [15]. This technique was used to investigate the decays of $^{114-118}$Ba, and, in particular, to measure their half-lives and β-delayed proton (βp) properties [14]. However, the α and cluster emission from ^{114}Ba remained undetected, and only upper limits of 3.7×10^{-3} (68% c.l.) [12] and 3.4×10^{-5} (84% c.l.) [13] could be determined for the respective decay branching ratios. By using the same method under improved conditions, it seemed possible to detect the α-decay of ^{114}Ba and thus to determine the corresponding b_α-value and reduced width for this nucleus, as well as for its daughter and granddaughter nuclei ^{110}Xe and ^{106}Te.

The comparatively high ^{114}Ba^{19}F$^+$ intensity obtained in our previous work [14] is an obvious motivation to search for the next lighter, hitherto unobserved barium isotope ^{113}Ba. Mass formulae predict for this nucleus positive Q_α values of 4.02 MeV [16] or 3.41 MeV [11]. The isotope ^{113}Ba is expected to be bound for one-proton emission, and unbound against two-proton emission. The one-proton separation energy (S_p) and two-proton separation energy (S_{2p}) of this "proton drip-line" nucleus are predicted to be only 50 and -710 keV [16], 680 and -560 keV [11], respectively. Given the uncertainties of such predictions, direct one-proton and two-proton decays may be energetically possible, and may thus compete with β-decay and direct α emission.

We report here on a re-investigation of the decay of ^{114}Ba and a search for ^{113}Ba, performed at the GSI on-line mass separator. The details of these measurements are described in the next section, followed by a presentation of the experimental results in Section 3, their discussion in Section 4, and a summary in Section 5.

2. Experimental technique

The ^{113,114}Ba atoms were produced at the GSI on-line mass separator by means of ^{58}Ni(^{58}Ni, $3n$) and ^{58}Ni(^{58}Ni, $2n$) fusion-evaporation reactions. During the course of the experiment, the average intensity of the ^{58}Ni beam amounted to 36 particle-nA; its energy was 284 MeV for the ^{113}Ba production and varied between 222 and 248 MeV during the ^{114}Ba measurement; the thickness of the highly enriched ^{58}Ni targets ranged from 2.0 to 3.8 mg/cm^2. The cross section was measured to be $0.20^{+0.13}_{-0.09}$ µb [14] for ^{114}Ba, while it is predicted by the HIVAP code [17] to be 5 µb. The same code predicts only 0.07 µb for ^{113}Ba.

The targets were positioned on a wheel in front of the ion source of the mass separator and could be exchanged by remote control when the monitor measurements, discussed below, showed signs of target degradation. After passage through thin heat shields and the window of the ion source, the recoiling reaction products were stopped inside the ion source in two tantalum foils of about 3 mg/cm^2 each. At the ion-source temperature of around 2400 K, the barium recoils are swiftly released from the thin catchers as thermalized atoms.

As ion source we used the high-temperature cavity source [18] with on-line fluorination by CF_4 addition. As it was proven in our previous studies of light barium isotopes [13,14], this type of source offers good ionization efficiency ($\sim 10\%$ for ^{114}Ba, see [19]) as well as a high degree of reliability and reproducibility, and—above all—it ionizes in the fluoride sideband selectively BaF^+, all contaminations including CsF^+ being reduced to levels well below 10^{-5} [19]. The CF_4 was introduced from a test leak with a flow of 2.2×10^{-6} std cm^3/s. This ensures efficient fluorination as indicated by the continuously controlled BaF^+/Ba^+ ratio of 14 ± 4, the variation reflecting the scatter that occurred for the three ion sources used throughout this experiment.

The ions, extracted from the source, were accelerated to 55 keV and mass-separated. The resulting beams of $^{113}Ba^{19}F^+$ ($A = 132$) and $^{114}Ba^{19}F^+$ ($A = 133$) were investigated by means of decay spectroscopy. The latter had an intensity of 4 atoms/min, as deduced from the decay radiation discussed below. The mass-separated beam of interest was alternately implanted in two 29 $\mu g/cm^2$ thick carbon foils which were each viewed by a telescope. The implantation intervals were chosen as 1 and 4 s for $A = 132$ and $A = 133$, respectively. Each of the telescopes covered $(34 \pm 3)\%$ of 4π sr, and consisted of two silicon surface-barrier detectors for recording energy-loss (ΔE) and rest energy (E) of protons and α particles. The ΔE detectors had an area of 450 mm^2 and thickness of 20.1 and 22.5 µm, while the corresponding dimensions of the E detectors were 2000 mm^2 and 500 µm thick. The energy calibration of the detectors was achieved by using ^{148}Gd, ^{241}Am, ^{239}Pu and ^{244}Cm α sources. The energy resolution obtained for 3184 keV α particles in the ΔE and E detectors amounted to 97 and 48 keV, respectively, for the telescope with the thinner ΔE detector, and 84 and 55 keV, respectively, for the other telescope.

Energy and time signals from the ΔE and E detectors were recorded in event by event mode, with the dead time after each accepted trigger extending to about 100 µs.

The identification of β-delayed protons (βp) and α particles ($\beta\alpha$), emitted from the implanted activity, was accomplished on the basis of ΔE–E scatter plots for the two telescopes. By selecting areas in these plots, energy spectra for high-energy βp events were obtained by coincident summation of ΔE and E signals. These areas were verified in a separate online measurement of clean ^{114}Cs sources [21], which were prepared by using a high-temperature cavity source without fluorination. During the main experiment, based on the $^{114}Ba^{19}F^+$ beam, the βp rate detected for $A = 133$ was used to monitor the overall performance of the experiment, with ^{114}Cs contributing as a daughter activity. In this context, and throughout this entire Letter, the weak branching ratio for β-delayed α emission of ^{114}Cs, $(1.6 \pm 0.6) \times 10^{-3}$ [21], is neglected. The βp data obtained for ^{114}Ba agree with respect to energy spectrum and half-life with those obtained earlier [14], and will not be discussed further in this Letter. During the search for ^{113}Ba at $A = 132$, a monitor measurement was carried out at mass 133 at another beam-line of the on-line mass separator, where a separate pair of telescopes was installed, and was based on the detection of βp activity from ^{114}BaF.

In addition to the ΔE–E scatter plots, based on events recorded in coincidence between the two detectors of a telescope, low-energy events from βp as well as direct proton and α-decay can be searched for in the energy spectra of the ΔE detectors, accumulated in anticoincidence with the accompanying E detector. The anticoincidence condition serves to suppress energy-loss events of positrons and high-energy βp radiation. In this operation mode, the maximum energy deposited by protons or α particles, which approximately corresponds to their range in silicon, varied from 1.2 to 2.2 MeV for protons [22] and 4.4 to 8.8 MeV for α particles [22] in the case of the telescope with the thinner ΔE detector. For the other telescope, the corresponding values are 1.3 to 2.4 MeV and 4.8 to 9.4 MeV [22], respectively. These ranges of maximum energies are related to the different angles of incidence, given by the source-telescope geometry.

Information on the half-lives of the implanted ions and their daughter activities can be gained in two ways. First, the grow-in/decay time-spectra of ΔE–E coincidence or ΔE–E anticoincidence events can be used, when generated as a function of the time elapsed within the implantation intervals of 1 and 4 s for ^{113,114}Ba, respectively. Second, the half-life of the respective daughter isotope can be found by evaluating the time correlations between consecutive decay-events. This method was applied to analyse ^{114}Ba and ^{110}Xe α decays.

From the intensities of the α lines in the ^{114}Ba–^{110}Xe–^{106}Te–^{102}Sn decay chain, the b_α values for ^{114}Ba and ^{110}Xe can be deduced by taking into account corrections for the recoil escape. The probability that ^{110}Xe and ^{106}Te recoils are ejected from the carbon foil after α-decay of ^{114}Ba and ^{110}Xe was calculated [22] to be 27% and 20%, respectively. The recoil-escape probability is higher if one considers observation of two consecutive decays in the α-chain. In such cases, the detection of the first α-decay means that the recoil is emitted in the opposite direction and has high chance of being ejected from the carbon foil. The detection of ^{114}Ba α-decay implies 71% escape probability of ^{110}Xe recoil. In the events in which α decay of ^{110}Xe was observed, about 49% of the ^{106}Te atoms recoiled out from the foil.

Total counting times of 10 and 55.6 h were devoted to the measurements at $A = 132$ and $A = 133$, respectively. In the latter case, this corresponds to an improvement of the experimental sensitivity by a factor of 2.5 compared to our previous work [12], taking the ^{114}Ba^{19}F intensity, the detection efficiency and the counting time into account.

3. Results

3.1. *Alpha decay of* ^{114}Ba, ^{110}Xe *and* ^{106}Te

3.1.1. *Alpha-particle energies*

Fig. 1 displays the 2000 to 5000 keV section of the energy spectrum that was accumulated at $A = 133$ in the ΔE detectors of both telescopes in anticoincidence with the related E detectors. This spectrum contains events due to the energy loss of particles that were either stopped in the ΔE detectors or passed them without triggering the related E detectors. Three peaks can be identified in this picture, with energies of 3410, 3730 and 4160 keV. We interpret them as being due to α-decay, as βp radiation of such an energy would pass through the ΔE detector (see Section 2) and stop in the E detector, thus appearing in the coincidence and not in the anticoincidence spectrum. In contrast, α particles of this energy are stopped in the ΔE detector (see Section 2), thus appearing only in the anticoincidence spectrum. The events occurring around 2.2 to 2.4 MeV in the spectrum shown in Fig. 1 may partly be due to βp radiation, as these energies correspond to the maximum ranges in the ΔE detectors (see Section 2). The total number of events, found for the members of the triplet shown in Fig. 1, amount to 39, 18 and 15, respectively. Because of the lower experimental sensitivity (see Section 2), the previous measurement [12] did not yield unambiguous evidence for the triplet, neither for the strongest lower-energy line.

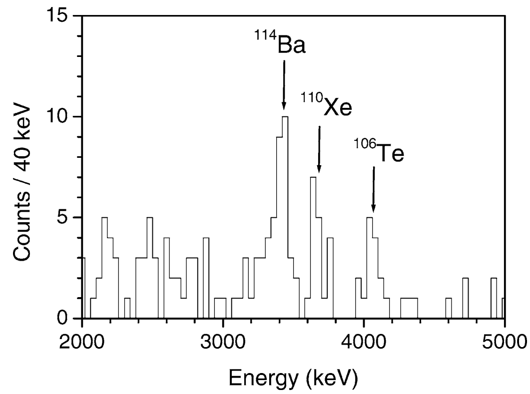

Fig. 1. Section of the ΔE spectrum from both telescopes, taken in anticoincidence with the related E detectors and corrected for background. The peaks assigned to the α-decays of ^{114}Ba, ^{110}Xe and ^{106}Te are marked. The events between 2000 and 2400 keV are assigned to low-energy βp that are stopped in the ΔE detector (see text for details).

The lowest-energy line, with an E_α value of 3410 ± 40 keV, is assigned to the α-decay of ^{114}Ba. The higher-energy members of the triplet are interpreted as being due to the known [20,23,24] α lines of the daughter ^{110}Xe and the granddaughter ^{106}Te. This assignment is based on the Z and A selectivity reached by combining the fluorination ion-source with mass separation (see Section 2). Within the respective uncertainties, the E_α values found in this work for the latter two cases,

3730 ± 30 and 4160 ± 30 keV, respectively, agree with the literature values (3745 ± 14 keV [23] and 4128 ± 9 keV [24]), which, however, are more accurate. In Table 1, the E_α data are listed together with the Q_α, determined by taking the recoil correction into ac-

Table 1
Experimental α-decay properties of ^{114}Ba, ^{110}Xe and ^{106}Te. Except for the cases indicated by literature references, the data stem from this work (see text for details)

Nucleus	$T_{1/2}$ (ms)	b_α (%)	E_α (keV)	Q_α (keV)	W_α
^{114}Ba	430^{+300}_{-150} [14]	0.9±0.3	3410±40	3540±40	16^{+12}_{-7}
^{110}Xe	160^{+290}_{-60}	64±35	3745±14 [23]	3885±14 [23]	$1.6^{+3.0}_{-1.0}$
^{106}Te	$0.060^{+0.030}_{-0.010}$ [20]	100	4128±9 [24]	4290±9 [24]	$5.1^{+2.6}_{-0.9}$

count, as well as the experimental results on half-life (see Section 3.1.3), b_α (see Section 3.1.2) and reduced width relative to ^{212}Po, W_α (see Section 4.2).

3.1.2. Alpha-decay branching ratios

The b_α values for ^{114}Ba and ^{110}Xe can be deduced from the intensities of the α lines in the ^{114}Ba–^{110}Xe–^{106}Te–^{102}Sn decay chain. The b_α value of ^{114}Ba was determined to be $(9 \pm 3) \times 10^{-3}$ by comparing the 39 events, assigned to this disintegration mode, with the 980βp events detected simultaneously in ΔE–E coincidence. This evaluation takes into account also the detection efficiency of the telescopes (see Section 2) and the previously determined [13] ratio of 25 ± 7 between the number of ^{114}BaF ions implanted in the carbon stopper foils and the number of βp events recorded in two telescopes of (17 ± 2)% efficiency each. The new b_α value of ^{114}Ba is somewhat larger than but still compatible with the previously obtained upper limit of 3.7×10^{-3} (64% c.l.) [12].

The b_α for ^{106}Te has been assumed to 100%, since for a half-life of 60 µs a β-decay contribution can be neglected, and the uncertainty of this assumption is small compared to the half-life uncertainty. Since the energy of the implanted ^{114}BaF ions is about 2.5 times lower than the energy gained by the recoils after α-decay of ^{114}Ba and ^{110}Xe, the decay products can escape the detection system by being ejected from the carbon foil backwards with respect to the beam direction. These values were taken into account in the evaluation of the α-decay branching ratio. The b_α value for ^{110}Xe was determined to be (64 ± 35)% by assuming that $b_\alpha(^{114}\mathrm{Ba}) = (9 \pm 3) \times 10^{-3}$ and $b_\alpha(^{106}\mathrm{Te}) = 100\%$. The b_α results are listed in Table 1.

3.1.3. Half-lives

The unknown half-life of ^{110}Xe was determined through the analysis of time correlations between ^{114}Ba and ^{110}Xe–^{106}Te α-decay events. The 60 µs half-life of ^{106}Te allows to consider the decays of ^{110}Xe and ^{106}Te as prompt events in a time scale which can be estimated from the known α-decay energy of ^{110}Xe. For this reason we looked for correlations between ^{114}Ba α-decay and ^{110}Xe or ^{106}Te events. This analysis yielded two events that have a time difference from the ^{114}Ba detection of 248 and 214 ms, respectively. The mean lifetime of ^{110}Xe was calculated as the average of these two values [25]. The prerequisites for applying this method are that the measurement covered the full time range, i.e., the measurement is sensitive to very small and very large decay times compared with the half-life of interest, and that contributions from other radioactive species and room background are negligible [25]. If we consider the lower limit of 100 µs from the dead-time of the data acquisition system, the upper limit of more than 1 h (average time difference between two α decays of ^{114}Ba) and that contamination can most probably be neglected, the conditions of our measurement fulfill both the requirements for applying the method. These considerations yielded a value of 230^{+420}_{-90} ms for the mean lifetime of ^{110}Xe and thus $T_{1/2} = 160^{+290}_{-60}$ ms. The uncertainties are calculated according to [26] for an exponential distribution.

The results of the time correlated events confirm the above-mentioned assignment of the 3410 keV α line to ^{114}Ba. As the work presented here did not improve the half-life results for ^{114}Ba and ^{106}Te, these values were taken from previous works (see Table 1).

3.2. Search for ^{113}Ba

The search for ^{113}Ba was performed by using also the fluorination method and selecting mass 132. During a total measuring time of 10 h, no clear evidence for ^{113}Ba β- or α-decay was found; on the basis of this “result”, we are unable to draw unambiguous conclusions concerning production cross section, half-life and decay properties of ^{113}Ba.

4. Discussion

4.1. Q_α and $Q_{^{12}\mathrm{C}}$ values

The Q_α values along an α-decay chain generally *decrease*, e.g., for the chain ^{174}Pt to ^{154}Er from 6.2 to 4.2 MeV [10]. However, when an α-decay chain ends in a doubly-magic nucleus or close to it, the inverse effect occurs due to the extra binding energy of nuclei in the vicinity of double magicity. For example, the Q_α values *increase* along the α chain from ^{232}Pu to ^{208}Pb from 6.7 to 9.0 MeV [10]. For the same reasons the increase of the E_α values along the triple α-chain, that starts from ^{114}Ba and ends in proton magic ($Z = 50$) ^{102}Sn (see Fig. 1), is an excellent example of experimental evidence for the $Z = 50$, $N = 50$ shell closure. In Fig. 2, experimental and theoretical Q_α values for tellurium, xenon and barium isotopes are displayed as a function of the neutron number. As far as predictions are concerned, we have chosen, as a representative sample, the finite-range droplet model (FRDM) [16], the semiempirical shell-model mass equation [11], and the relativistic Hartree–Bogoliubov (RHB) [27–29] model. The RHB calculations were performed in an axially deformed configuration applying the parameter set NL3 [30] for the relativistic Lagrangian while in the particle-particle channel the pairing part of the finite range Gogny force D1S [31] was used.

On the one hand, the FRDM [16] predicts the Q_α value of ^{114}Ba to be 3550 keV, i.e., very close to the experimental result, but yields Q_α values for ^{110}Xe and ^{106}Te that are too large by 720 and 1720 keV, respectively. This microscopic-macroscopic model apparently overestimates the shell strength at $Z = N = 50$. The semiempirical shell-model mass equation [11], on the other hand, reproduces very well the experimental Q_α values for $^{106-110}$Te and underestimates the values of $^{110-113}$Xe and ^{114}Ba by only about 300 keV. This mass equation is well known for reproducing also the experimental S_p values close to the shell closure $Z = N = 50$.

The RHB calculations yield Q_α values of 3730 keV for ^{114}Ba, i.e., about 200 keV larger than the experimental one, and of 4920 and 6210 keV for ^{110}Xe and ^{106}Te, respectively. This overestimation of 1035 and 1920 keV in the latter two cases is probably related to the fact that the RHB method is based on the mean-field approximation which is known to fail in transitional regions. The chain of nuclei ^{102}Sn, ^{106}Te, ^{110}Xe, ^{114}Ba starts close to the doubly-magic nucleus ^{100}Sn. As one leaves this region and adds more and more particles, additional correlations develop. Close to the magic core, i.e., at the lower end of the chain, one has a spherical potential and these correlations cannot be taken into account at all in the mean-field approach. Here we observe dramatic deviations form the experiment. With an increasing number of valence particles such correlations cause a transition to deformed shapes. Thus the mean-field approach can describe these correlations at least in an average way within the framework of deformed Slater determinants. In fact, we find in our calculations increasing quadrupole deformation parameters in the chain, i.e., $\beta = 0.14$ for ^{106}Te, $\beta = 0.20$ for ^{110}Xe, and $\beta = 0.27$ for ^{114}Ba. This explains at least qualitatively why the mean-field results show increasing agreement with the experimental data if we leave the spherical region. At present it is not clear whether one has to consider only quadrupole correlations leading to shape transitions. In addition one could think of proton–neutron (pn) pairing correlations or genuine four-particle correlations in quartet configurations. The pn-pairing correlations are expected to be important close to the $N = Z$ line,

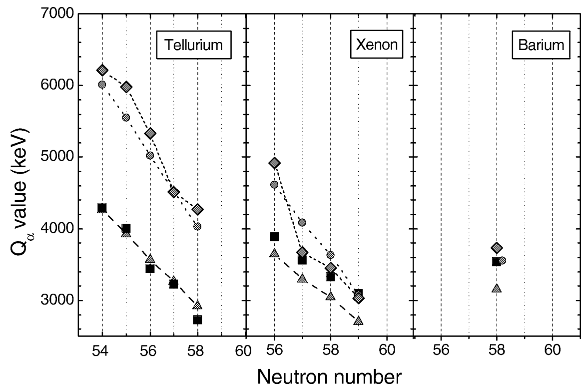

Fig. 2. Comparison of experimental Q_α values (full squares) for tellurium, xenon and barium isotopes, with predictions obtained from the FRDM model [16] (dotted line and circles), the semiempirical mass formula [11] (dashed line and triangles) and the RHB model (diamonds).

but have not been taken into account in the present calculations. These arguments would also explain that both the RHB as the FRDM calculations show similar deviations from the experimental values, because both of them are based on the mean-field approximation and do not include pn-pairing nor quartet correlations.

By summing the three Q_α values and correcting for the binding energies of the three α particles and ^{12}C, we deduced an experimental $Q_{^{12}\mathrm{C}}$ of ^{114}Ba of 19.00 ± 0.04 MeV, which is just below the upper limit of 19.3 MeV from a previous empirical estimate [13]. The FRDM and RHB calculations overestimate the $Q_{^{12}\mathrm{C}}$ by 2.44 MeV [9] and 3.14 MeV, respectively, while the semiempirical shell-model mass equation underestimates it by 0.66 MeV [11]. As already mentioned in Section 1, the knowledge of this value is important in order to obtain experimentally relevant predictions from cluster-emission calculations, as the partial half-life for ^{12}C emission depends dramatically on the adopted $Q_{^{12}\mathrm{C}}$ value. By considering a $Q_{^{12}\mathrm{C}}$ of 19.0 MeV, the most widely used theoretical models [7,8] predict partial half-lives for ^{12}C decay of ^{114}Ba that are 6 and 4 orders of magnitude above the experimentally established upper limit (1.2×10^4 s [13]).

4.2. Systematics of α-decay widths

The reduced α-decay width can either be expressed as a parameter δ^2 (in MeV) due to the relation

$$\delta^2 = h \cdot \frac{\lambda_\alpha}{P}, \tag{1}$$

where h is the Planck constant, λ_α the partial decay constant for α-decay and P the penetration probability, or by the dimensionless quantity W_α, which is defined relative to that for ^{212}Po ground-state α-decay ($\delta^2/\delta^2(^{212}\mathrm{Po})$) [1]. By using the newly determined E_α, b_α and half-life results described in Section 3, we deduced the W_α values of ^{114}Ba, ^{110}Xe and ^{106}Te and thus extend the W_α systematics towards its low-mass end [1] (see Table 1). The reduced width of the ^{114}Ba α-decay of 16^{+12}_{-7} is somewhat larger than, but within error bars consistent with the W_α values of $1.6^{+3.0}_{-1.0}$ and $5.1^{+2.6}_{-0.9}$ found for ^{110}Xe and ^{106}Te, respectively. Hence, the large uncertainties of the W_α values, listed in Table 1, prevent us from drawing any firm conclusion concerning superallowed α-decay.

5. Summary

By using the GSI on-line mass separator, we performed a search for ^{113}Ba and for the α-decay of ^{114}Ba. While the former measurement remained unsuccessful, we were able to identify for the first time the triple α-decay, linking the neutron-deficient isotopes ^{114}Ba and ^{102}Sn through ^{110}Xe and ^{106}Te. We measured the energy of the ^{114}Ba α particles to be 3410 ± 40 keV and determined the branching ratio $b_\alpha = (9 \pm 3) \times 10^{-3}$ and the α-decay width $W_\alpha = 16^{+12}_{-7}$. By means of the time correlation technique, we were also able to determine experimentally the hitherto unknown half-life of ^{110}Xe to be $T_{1/2} = 160^{+290}_{-60}$ ms.

The experimental Q_α and $Q_{^{12}\mathrm{C}}$ values of ^{114}Ba allowed us to improve estimates of the cluster decay half-life of this isotope. The large uncertainties of the W_α values, however, prohibited any firm conclusion concerning superallowed α-decay, which continues to be a challenge to future dedicated experiments.

Acknowledgements

The authors would like to acknowledge the valuable contributions of K. Burkard and W. Hüller to developing and operating the GSI on-line mass separator. G.A.L. wishes to thank GSI for financial support. This work was supported in part by the Polish Committee of Scientific Research, in particular, under Grant No. KBN 2 P03B 086 17, by the Programme for Scientific Technical Collaboration (WTZ) under Projects No. POL 99/009 and No. RUS 98/672, and by the European Community under Contracts No. ERBFMGECT950083 and No. HPRI-CT-1999-00001.

References

[1] E. Roeckl, Alpha decay, in: D.N. Poenaru (Ed.), Nuclear Decay Modes, Institute of Physics Publishing, 1996, p. 237.
[2] R.D. Macfarlane, A. Siivola, Phys. Rev. Lett. 14 (1965) 114.
[3] W. Greiner, M. Ivascu, D.N. Poenaru, A. Sandulescu, in: D.A. Bromley (Ed.), Treatise on Heavy Ion Science, Vol. 8, Plenum, New York, 1989, p. 641.
[4] D.N. Poenaru, D. Schnabel, W. Greiner, D. Mazilu, R. Gherghescu, At. Data Nucl. Data Tables 48 (1991) 231.

[5] S.G. Kadmenski, S.D. Kurgalin, N.L. Miheev, N.I. Furman, Yu.M. Chuvilski, Izv. Akad. Nauk. Rossii 57 (1993) 12.
[6] R. Blendowske, H. Walliser, Phys. Rev. Lett. 61 (1988) 1930.
[7] D.N. Poenaru, W. Greiner, R. Gherghescu, Phys. Rev. C 47 (1993) 2030.
[8] S. Kumar, R.K. Gupta, Phys. Rev. C 49 (1994) 1922.
[9] P. Möller, J.R. Nix, W.D. Myers, W.J. Swiatecki, At. Data Nucl. Data Tables 59 (1995) 185.
[10] G. Audi, O. Bersillon, J. Blachot, A.H. Wapstra, Nucl. Phys. A 624 (1997) 1.
[11] S. Liran, N. Zeldes, At. Data Nucl. Data Tables 17 (1976) 431.
[12] A. Guglielmetti, R. Bonetti, G. Poli, P.B. Price, A.J. Westphal, Z. Janas, H. Keller, R. Kirchner, O. Klepper, A. Piechaczek, E. Roeckl, K. Schmidt, A. Płochocki, J. Szerypo, B. Blank, Phys. Rev. C 52 (1995) 740.
[13] A. Guglielmetti, R. Bonetti, G. Poli, R. Collatz, Z. Hu, R. Kirchner, E. Roeckl, N. Gunn, P.B. Price, B.A. Weaver, A. Westphal, J. Szerypo, Phys. Rev. C 56 (1997) R2912.
[14] Z. Janas, A. Płochocki, J. Szerypo, R. Collatz, Z. Hu, H. Keller, R. Kirchner, O. Klepper, E. Roeckl, K. Schmidt, R. Bonetti, A. Guglielmetti, G. Poli, A. Piechaczek, Nucl. Phys. A 627 (1997) 119.
[15] K. Schmidt, R. Borcea, K. Burkard, J. Döring, M. Górska, H. Grawe, W. Hüller, Z. Janas, R. Kirchner, M. La Commara, C. Mazzocchi, E. Roeckl, in: U. Köster (Ed.), Proc. 5th Conf. on Radioactive Nuclear Beams, Divonne, April 2000, Nucl. Phys. A, in print.
[16] P. Möller, J.R. Nix, K.-L. Kratz, At. Data Nucl. Data Tables 66 (1997) 131.
[17] W. Reisdorf, Z. Phys. A 300 (1981) 227.
[18] R. Kirchner, Nucl. Instrum. Methods Phys. Res. A 292 (1990) 203.
[19] R. Kirchner, Nucl. Instrum. Methods Phys. Res. B 126 (1997) 135.
[20] D. Schardt, T. Batsch, R. Kirchner, O. Klepper, W. Kurcewicz, E. Roeckl, P. Tidemand-Petersson, Nucl. Phys. A 368 (1981) 153.
[21] E. Roeckl, G.M. Gowdy, R. Kirchner, O. Klepper, A. Piotrowski, A. Płochocki, W. Reisdorf, P. Tidemand-Petersson, J. Żylicz, D. Schardt, G. Nyman, W. Lindenzweig, Z. Phys. A 294 (1980) 221.
[22] J.P. Biersack, J.F. Ziegler, SRIM 2000, http://www.research.ibm.com/ionbeams/SRIM/SRIMFULL.exe.
[23] G. Audi, A.H. Wapstra, Nucl. Phys. A 565 (1993) 66.
[24] R.D. Page, P.J. Woods, R.A. Cunningham, T. Davinson, N.J. Davis, A.N. James, K. Livingston, P.J. Sellin, A.C. Shotter, Phys. Rev. C 49 (1994) 3312.
[25] K.-H. Schmidt, Eur. Phys. J. A 8 (2000) 141.
[26] K.-H. Schmidt, C.-C. Sahm, K. Pielenz, H.-G. Clerc, Z. Phys. A 316 (1984) 19.
[27] G.A. Lalazissis, D. Vretenar, P. Ring, Phys. Rev. C 57 (1998) 2294.
[28] G.A. Lalazissis, D. Vretenar, P. Ring, Phys. Rev. C 63 (2001) 034305.
[29] G.A. Lalazissis, D. Vretenar, P. Ring, Nucl. Phys. A 650 (1999) 133.
[30] G.A. Lalazissis, J. König, P. Ring, Phys. Rev. C 55 (1997) 540.
[31] J.F. Berger, M. Girod, D. Gogny, Nucl. Phys. A 428 (1984) 32.